Winner of the 2000 Excellence in Research Award

Biomechanical Properties and Vascularity of an Anterior Cruciate Ligament Graft Can Be Predicted by Contrast-Enhanced Magnetic Resonance Imaging

A Two-Year Study in Sheep*

Andreas Weiler,†‡ MD, Gunnar Peters,† CM, Jürgen Mäurer,§ MD,
Frank N. Unterhauser,† MD, and Norbert P. Südkamp,† MD

From the †Trauma and Reconstructive Surgery, Sports Traumatology and Arthroscopy Service and §Department of Radiology, Charité, Campus Virchow-Clinic, Humboldt-University of Berlin, Germany

ABSTRACT

Magnetic resonance imaging has been used to determine graft integrity and study the remodeling process of anterior cruciate ligament grafts morphologically in humans. The goal of the present study was to compare graft signal intensity and morphologic characteristics on magnetic resonance imaging with biomechanical and histologic parameters in a long-term animal model. Thirty sheep underwent anterior cruciate ligament reconstruction with an autologous Achilles tendon split graft and were sacrificed after 6, 12, 24, 52, or 104 weeks. Before sacrifice, all animals underwent plain and contrast-enhanced (gadolinium-diethylenetriamine pentacetic acid) magnetic resonance imaging (1.5 T, proton density weighted, 2-mm sections) of their operated knees. The signal/noise quotient was calculated and data were correlated to the maximum load to failure, tensile strength, and stiffness of the grafts. The vascularity of the grafts was determined immunohistochemically by staining for endothelial cells (factor VIII). We found that high signal intensity on magnetic resonance imaging reflects a decrease of mechanical properties of the graft during early remodeling. Correlation analyses revealed significant negative linear correlations between the signal/noise quotient and the load to failure, stiffness, and tensile strength. In general, correlations for contrast-enhanced measurements of signal intensity were stronger than those for plain magnetic resonance imaging. Immunohistochemistry confirmed that contrast medium enhancement reflects the vascular status of the graft tissue during remodeling. We conclude that quantitatively determined magnetic resonance imaging signal intensity may be a useful tool for following the graft remodeling process in a noninvasive manner.

Magnetic resonance imaging is widely accepted as the imaging procedure of choice for depicting internal derangements of the knee joint, especially for allowing accurate evaluation of tears of the native ACL.[31,33,37,44,46,51,52] Although the use of MRI to diagnose ACL ruptures is well established, several clinical studies have reported vastly different data on graft visibility and the prediction of graft integrity using MRI scans with plain and gadolinium-diethylenetriamine pentacetic acid (Gd-DTPA) enhanced imaging after ACL reconstruction or repair.[1,3,11,15,16,20,22–24,34,38–40,45,49,50,53,58] However, this may be due to different imaging techniques, different reconstructive procedures, and the possible effect of graft impingement by the intercondylar roof.[19,21,22] In the past, only a few studies have investigated ACL graft maturation by the use of MRI in humans.[4,20,23,48,54] The objective of these studies was to use MRI to follow the graft remodeling process in humans in a noninvasive way. But no data exist that correlate MRI findings, such as signal intensity or signal homogeneity of the graft, with

biomechanical or histologic parameters during early and late graft remodeling.

We performed a 2-year animal study to evaluate the fate of an ACL graft with MRI, biomechanical testing, and histologic evaluation to answer the following research questions: 1) Do changes in MRI signal intensity reflect the process of graft remodeling as determined by biomechanical and histologic parameters? 2) Do quantitative MRI parameters, such as signal intensity, predict biomechanical graft properties? 3) Does the infusion of Gd-DTPA improve visibility of the graft on MRI? and 4) Does the degree of contrast medium enhancement reflect graft vascularity on MRI?

MATERIALS AND METHODS

Study Design and Operative Procedure

Thirty skeletally mature female merino sheep were used in this study. The animals underwent replacement of the ACL in the left hindlimb using an Achilles tendon split graft with biodegradable interference screw fixation. All animals were screened to ensure good physical condition. All procedures were performed with permission of the local governmental animal rights protection authorities in accordance with the National Institutes of Health guidelines for the use of laboratory animals.

Five groups were assigned and animals were sacrificed at 6, 12, 24, 52, or 104 weeks. Each group consisted of six specimens. For biomechanical testing, 12 contralateral knees with intact ACLs served as control specimens. Ten contralateral reconstructed knees and 12 Achilles tendon split grafts were tested as time zero controls. Testing of contralateral knees was performed after sacrifice. Before the animals were sacrificed, MRI scans of the operated left knees were taken in all animals. For control, MRI scans of the nonoperated contralateral right knees were obtained in six animals of the 6-week group.

Anesthesia was induced intravenously with thiopental sodium. After the animal was intubated, anesthesia was maintained with isoflurane and nitrous oxide. The left hindlimb was shaved and prepared in the standard sterile fashion. The calcaneus communis tendon was exposed through a posterolateral skin incision, and the Achilles tendon was carefully separated from the flexor digitorum longus tendon. Half of the Achilles tendon, 7.5 cm in length, was sharply dissected. The incision was closed in layers using polyglactin and polyamidic sutures. Number 2 Ethibond sutures (Ethicon, Inc., Somerville, New Jersey) were passed through both ends of the Achilles tendon graft in a modified Bunnel stitch, and the graft was then kept moist in saline-soaked gauze.

The knee joint was exposed through an anteromedial incision. The patella was displaced laterally, the infrapatellar fat pad was sharply separated, and the plica synovialis and the ACL were exposed and removed. To avoid the use of a drill guide, we drilled a 6-mm tunnel at the original tibial insertion site of the ACL from inside to outside with the knee in 90° of flexion. The tunnel was then enlarged by dilatation with a 7-mm dilator, and the

cortical bone at the tunnel entrance was carefully chamfered to a diameter of approximately 8 mm. With the knee in maximum flexion, the femoral tunnel was created in the 1-o'clock position in the same fashion, leaving approximately 2 mm of the dorsal femoral cortex. The graft was then inserted via the holding sutures using a Beath pin.

The biodegradable interference screw consisted of poly-(D,L-lactide) (Sysorb, Sulzer Orthopedics Ltd., Baar, Switzerland). A biodegradable interference screw was chosen because the use of these implants has recently gained favor for direct soft tissue graft fixation and because they allow for undistorted MRI.[5, 10, 36, 47, 55, 57]

With the graft tensioned from both sides, the first interference screw was inserted in the femoral tunnel. The knee was then taken through 10 full ranges of motion under 90 N of graft pretensioning using a tensiometer (Sulzer Orthopedics Ltd.). The tibial screw was inserted in an inside-out direction at 90° of flexion under pretension with 90 N. Finally, graft impingement at the intercondylar roof was carefully checked with a probe with the knee in full extension. The incision was closed using polyglactin and polyamidic sutures. The animals were then returned to their cages and were allowed to bear full weight immediately.

MRI Protocols

Before sacrifice, all animals were anesthesized and intubated using thiopental sodium intravenously so that MRI scans could be made in vivo. The MRI scans were performed using a 1.5-T super-conducting magnet (Siemens Magnetom 63 SP, Siemens AG, Erlangen, Germany) with a dedicated surface coil (Siemens AG). Imaging was confined to 2-mm thick oblique (10° to 15°), sagittal sections centered about the intercondylar region of the knee in 90° of flexion. Proton density-weighted images were acquired with the standard spin-echo technique (1000 msec repetition time and 20 msec echo delay time). After intravenous infusion of 0.1 mmol/kg bodyweight Gd-DTPA (Prohance, Byk Gulden, Konstanz, Germany), image acquisition was repeated. Encoding and reconstruction was performed with the standard two-dimensional Fourier transformation technique, using a 256×256 matrix.

To quantitatively determine normalized signal intensity of the graft the signal/noise quotient (SNQ) was calculated[48]:

$$SNQ = \frac{signal(ACL\text{-}graft) - signal(PCL)}{signal(background)}$$

Circular 5-mm diameter regions of interest were evaluated at the midsubstance of the graft and close to the femoral and tibial insertion sites (Fig. 1). The PCL signal was measured with the region of interest placed in the midsubstance part of the ligament. For background measurements, the region of interest was placed approximately 2 cm anterior to the patellar tendon. Each measurement was performed three times and the average was recorded.
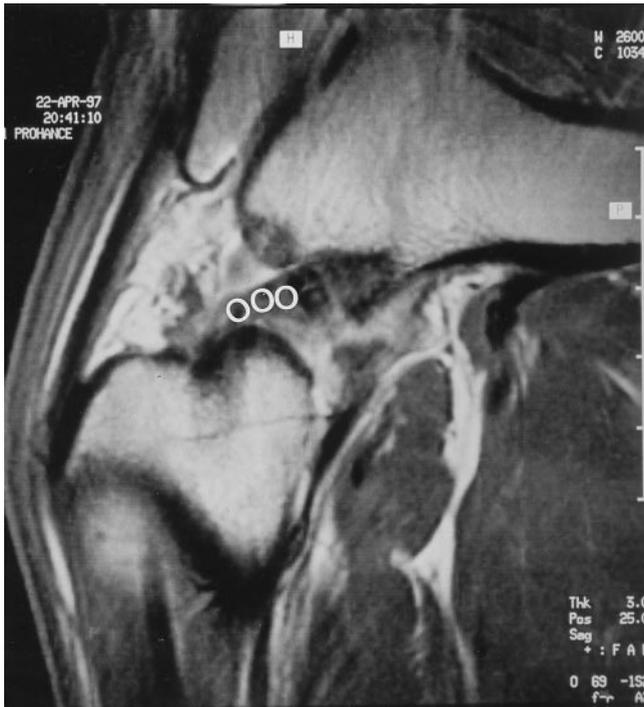
Figure 1. Oblique, sagittal MRI scan of an operated left knee showing the positions of the femoral, midsubstance, and the tibial regions of interest for signal intensity measurements.

Mechanical Testing

At 6, 12, 24, and 104 weeks, six specimens were included in each group, and in the 52-week group, five specimens were included in the final evaluation. In the 52-week group one specimen had to be excluded. All animals partially loaded their left hindlimb immediately after surgery and attained a normal gait within the first 2 weeks. Arthrotomy and tendon harvest sites healed without any complications in all animals.

Animals were sacrificed with an overdose of potassium chloride and thiopental sodium. The knees were harvested and wrapped in saline-soaked gauze and stored at $-20°C$ until testing. Twelve hours before testing, the knees were thawed at $4°C$. The tibial and femoral bone ends were cleaned of all remaining soft tissue and were embedded in aluminum cylinders using polymethyl methacrylate. All capsuloligamentous structures and the menisci were removed, leaving only the ACL graft. During all preparations and testing, specimens were kept moist with saline spray.

The tendon cross-sectional area was determined using an area micrometer (Mitutoyo Inc., Sakato, Japan) and a force transducer (± 0.1 N). To access the graft with different sized slots, the medial femoral condyle was resected. Each measurement was performed three times at the midsubstance portion of the graft at a force of 4.5 N and the average was recorded.

For biomechanical testing, specimens were mounted to a custom-made adjusting device that allows free rotation of the construct in different flexion angles.[12, 56] The ACL graft was carefully aligned parallel to the axis of the applied load in 60° of flexion. A preload of 1 N was applied and a load-to-failure test was performed at a displacement rate of 1 mm/sec. Stiffness and maximum load to failure were calculated from the load-displacement curve, and failure modes were recorded.

In addition to testing the reconstructed knees as time zero control specimens, 12 Achilles tendon split grafts were harvested from the contralateral limb to determine the structural properties of the graft tissue at time zero. After the cross-sectional area was determined,[17] the Achilles tendons were attached to a cryo-clamping device leaving a free tendon length of 3 cm between the clamps. The tendon ends were secured with blunt clamps and were deep frozen with dry ice. A preload of 5 N was applied, and specimens were then loaded until failure with a displacement rate of 1 mm/sec.

Immunohistochemistry

To determine the vascular status of the ACL graft, samples of approximately 5 mm were taken from the midsubstance of the graft and fixed in 5% formalin for 48 hours at room temperature. Because most grafts failed close to the femoral or tibial insertion sites during mechanical testing, an undisturbed midsubstance histologic evaluation was possible in all except two specimens. Samples were sliced into longitudinal sections and cross sections. Thereafter, specimens were dehydrated and embedded in paraffin. Four-micrometer thick sections were cut and mounted on slides coated with 3% silane (Sigma Chemical, St. Louis, Missouri). The paraffin was extracted and sections were rehydrated. Epitopes were unmasked by pretreating sections with 0.1% protease (Protease, Type XIV: Bacterial, Sigma-Aldrich Chemie GmbH, Steinheim, Germany) for 10 minutes at 37°C. Nonspecific binding of primary antibody was avoided by blocking sections with 10% normal horse serum (Vector Laboratories Inc., Burlingame, California). To detect endothelial cells of blood vessels, specimens were incubated overnight at 4°C with antihuman factor VIII (rabbit antihuman von Willebrandt factor, 1:200, Dako A/S, Glostrup, Denmark). After being rinsed in tris-buffered saline, tissues were incubated with biotinylated horse antirabbit IgG secondary antibody (Vector Laboratories Inc.) for 30 minutes at room temperature. Slides were again immersed in tris-buffered saline, after incubation for another 50 minutes with an avidin-biotin complex (ABC kit; Vector Laboratories Inc.) with alkaline phosphatase as a reporter enzyme. Staining was visualized using Neufuchsin as a chromogen. Cell nuclei were counterstained with methylen-green.

For conventional light microscopy, specimens were embedded in paraffin and stained with Masson-Goldner trichrome stain and hematoxylin and eosin.

Data Analysis

Biomechanical parameters and signal/noise quotient data were analyzed for equal distribution with the Kolmogoroff-Smirnov test. Because a nonparametric distribution was found, unpaired comparisons between the control groups and changes between the groups over time were performed using the Mann-Whitney U Wilcoxon rank sum test. Comparisons between scans before and after infusion with Gd-DTPA were made with the Wilcoxon test. The functional relationship between maximum load to failure, stiffness, and tensile strength and the signal/noise quotient data of the graft was determined using Spearman-Rho correlation analysis (α = 0.05). The probability level was set at $P \leq 0.05$.

RESULTS

Gross inspection of the knee joints at harvest showed that all grafts were covered by an intact synovial membrane with mild inflammatory changes, hypervascularization, and thickened synovial tissue. These changes were maximally pronounced at 6 weeks, but could not be detected at all after 12 weeks.

Biomechanics

Cross-sectional area measurements showed no significant difference between the graft at the time of reconstruction, the intact ACL, and the contralateral harvested graft for time-zero tensile testing (Table 1). Cross-sectional area decreased from time zero (24.4 ± 3.6 mm^2) to 6 weeks (18.9 ± 8.6 mm^2) (P = 0.041), indicating graft atrophy, whereas at 12 weeks the graft showed signs of hypertrophy (37.5 ± 7.5 mm^2) (P = 0.003) (Table 1).

All specimens at time zero failed by graft pullout from the tibial or femoral tunnel, whereas all specimens at 6 weeks failed at midsubstance. In the 6-week group, two specimens failed at the midsubstance portion of the graft and four near the femoral or tibial insertion sites. Failure mode after 12, 24, 52, and 104 weeks was osteocartilaginous avulsion at the tibial or femoral insertion site. At 104 weeks, two specimens failed in midsubstance and the remaining four by avulsion at the tibial insertion. Intact

contralateral ACLs failed either at midsubstance near the insertion sites or by femoral bony avulsion.

The mean tensile strength of the Achilles tendon split graft (39.8 ± 7.8 MPa) was 74.1% of that of the intact ACL (53.6 ± 13.6 MPa). The maximum load to failure of the time-zero reconstruction (267 ± 82 N) was 17.6% of the intact ACL (1513.3 ± 180.3 N). After 52 weeks, the mean tensile strength (25.4 ± 10.8 MPa) reached 63.8% and 47.3% that of the Achilles tendon split graft and the intact ACL, respectively, and a maximum load to failure (684.9 ± 252.8 N) of 61.2% and 44.7%, respectively (Table 1). In contrast, the mean maximum load to failure was 256.5% as opposed to the time-zero reconstruction. At 6 weeks tensile strength reached only 6.8% of the Achilles tendon split graft (2.7 ± 0.9 MPa) (Table 1). All tensile strength and maximum load-to-failure values between time zero and 104 weeks were significantly different from the Achilles tendon split graft and the intact ACL. All stiffness values between time zero and 52 weeks were significantly lower compared with the intact ACL (Table 1). At 6 weeks, stiffness of the graft was significantly lower than that of the time-zero femur-graft-tibia complex (14.4 ± 5.5 N/mm versus 41.2 ± 13 N/mm), and at 104 weeks stiffness values were significantly higher (99.5 ± 50 N/mm) (Table 1). All biomechanical data at 104 weeks were not significantly different from those at 52 weeks.

MRI and Histologic Findings

Six-Week Group. At 6 weeks, signal intensity of the graft was inhomogeneously distributed with hypo- and hyperintense areas (Fig. 2). Conventional light microscopy at that time showed zones of hypocellular nonremodeled graft tissue directly adjacent to hypercellular and hypervascularized reparative tissue invading the former graft tissue in columns (Fig. 3). Graft visibility on plain MRI scans was poor, but the infusion of Gd-DTPA led to a distinct contrast enhancement at the ventral synovial sheet surrounding the graft (Fig. 2). Factor VIII immunohistochemistry showed a distinct hypervascularity of the thickened synovial membrane and the subsynovial graft tissue, with only an inhomogeneously distributed and sporadic vascularized central part of the graft (Fig. 3).

TABLE 1
Results of Biomechanical Testing[a]

Time after surgery (weeks)	Maximum load to failure (N)	Stiffness (N/mm)	Cross-sectional area (mm^2)	Tensile strength (MPa)
0 (N = 10)	$267 \pm 82^{b,c}$	41.2 ± 13^b	24.4 ± 3.6	—
6 (N = 6)	$44.8 \pm 4^{b,c,d}$	$14.4 \pm 5.5^{b,d}$	$18.9 \pm 8.6^{b,c}$	$2.7 \pm 0.9^{b,c}$
12 (N = 6)	$237.8 \pm 59.8^{b,c}$	51.2 ± 11.2^b	37.5 ± 7.5	$6.3 \pm 1.1^{b,c}$
24 (N = 6)	$313.8 \pm 164.4^{b,c}$	58.6 ± 25.9^b	29.5 ± 9.8^c	$10.1 \pm 2.8^{b,c}$
52 (N = 5)	$684.9 \pm 252.8^{b,c,d}$	$90.5 \pm 30.3^{b,d}$	27.8 ± 7	$25.4 \pm 10.8^{b,c}$
104 (N = 6)	$669.7 \pm 283.3^{b,c,d}$	99.5 ± 50^d	25.3 ± 8.7	$23.2 \pm 8.7^{b,c}$
ACL (N = 12)	1531.3 ± 180.3^d	143.9 ± 16.1^d	35 ± 1.8	53.6 ± 13.6^c
Achilles tendon split graft (N = 12)	$1120.1 \pm 223.4^{b,d}$	—	27.9 ± 4.9	39.8 ± 7.8^b

[a] Data are given as means $\pm$ standard deviation.
[b] Significantly different from the intact ACL ($P \leq 0.05$); Mann-Whitney U Wilcoxon rank sum test.
[c] Significantly different from the Achilles tendon split graft ($P \leq 0.05$).
[d] Significantly different from the reconstruction at time zero ($P \leq 0.05$).
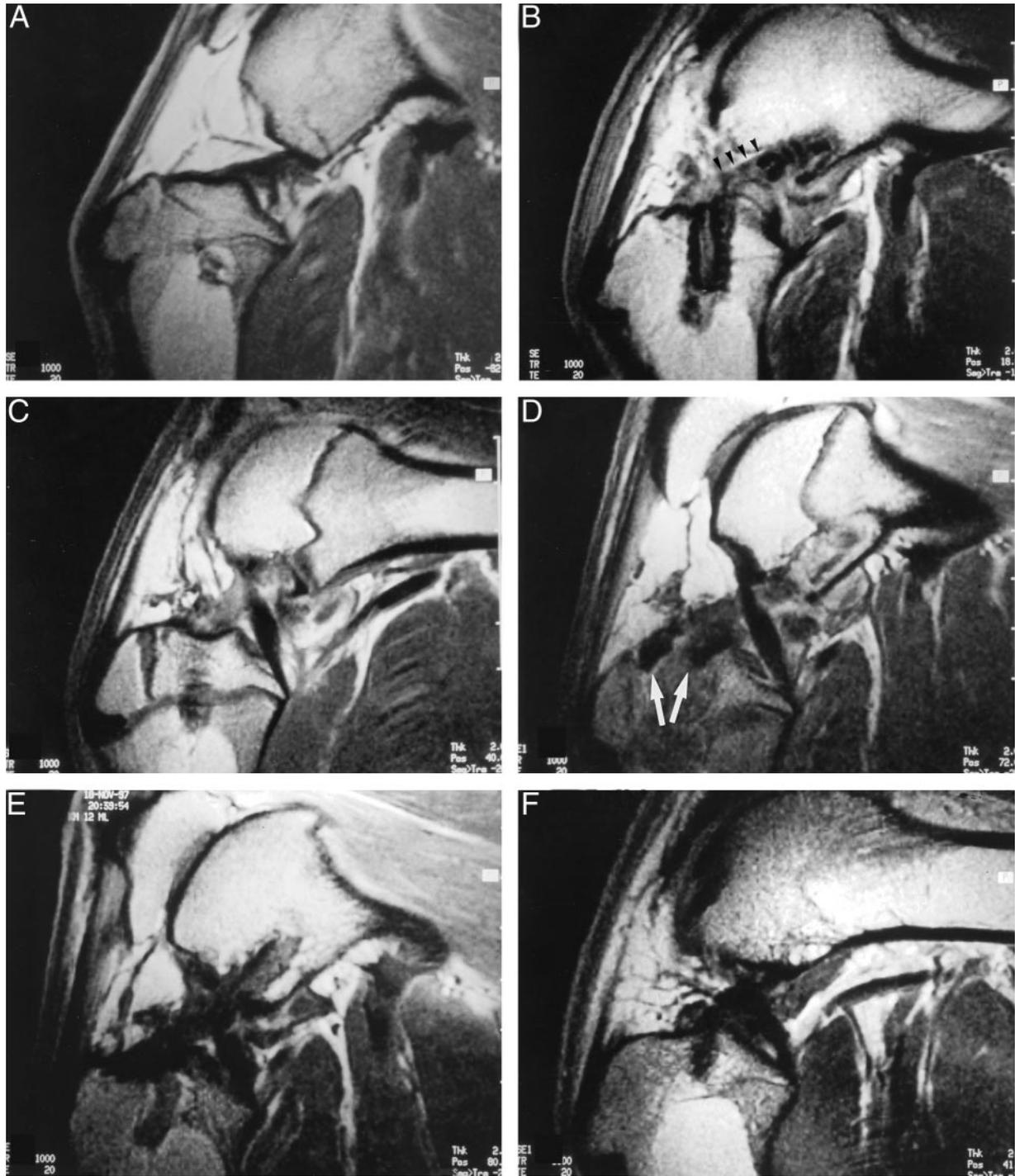
Figure 2. A, typical contrast-enhanced oblique sagittal MRI scan of the native ACL. B, at 6 weeks, signal intensity is inhomogeneously distributed with hypo- and hyperintense signal areas. Note the Gd-DTPA enhancement in the ventral synovial sheet (arrowheads). C, at 12 weeks there is a homogeneously distributed hyper- to isointense signal. D, at 24 weeks the graft appears iso- to hypointense. Note the low signal intensity at the tibial insertion site (arrows). E and F, at 52 (E) and 104 (F) weeks, the graft appears hypointense without any obvious Gd-DTPA enhancement.

Twelve-Week Group. At 12 weeks, signal intensity of the graft was hyper- to isointense and was homogeneously distributed compared with the 6-week group. Histologically, the graft still showed an increased amount of cells,

and the matrix was longitudinally orientated without a clear distribution into fascicles. Zones of nonremodeled former graft tissue could not be found at all. Graft visibility on plain MRI scans was still poor, but Gd-DTPA ap-
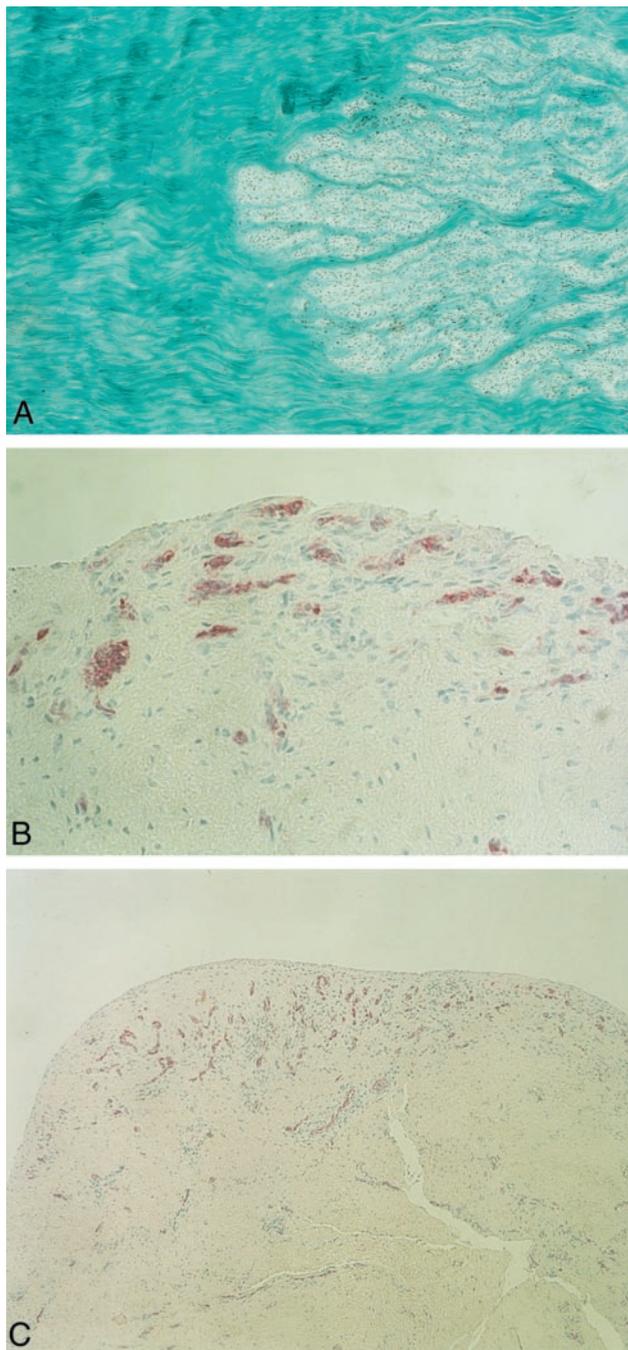
Figure 3. A, graft tissue at 6 weeks shows hypocellular tissue (left) invaded by hypercellular and vascularized repair tissue (right) (longitudinal section, Masson-Goldner trichrome stain). B, factor VIII immunohistochemistry shows a dense vascularized and thickened synovial membrane (transverse section, factor VIII immunostain). C, a lower magnification microphotograph shows subsynovial hypervascularity with only some vessels being visible at the central part of the graft (transverse section, factor VIII immunostain).

plication led to a homogeneous signal enhancement of the entire graft (Fig. 2). Factor VIII immunohistochemistry of the graft tissue showed a uniformly distributed hypervascularization with a markedly decreased vascularity of the synovial membrane and the subsynovial graft tissue (Fig. 4).

Twenty-four-Week Group. At 24 weeks, MRI signal intensity was iso- to hypointense. Signal intensity was especially low at the tibial graft insertion (Fig. 2). Histologically, the graft tissue was well structured and distributed into fascicles with a regular crimp (Fig. 5). The cell amount was markedly reduced compared with the 12-week group, and cells appeared fusiform (Fig. 5). The graft was easily visible on native MRI scans without an obvious improvement in visibility after Gd-DTPA infusion. Immunohistochemistry showed a distinct reduction in vascularity compared with the 12-week group. Vessels were distributed between graft fascicles. The number of vessels and their distribution was comparable with that of the native ACL (Fig. 5).

Fifty-two- and 104-Week Groups. Morphologically, there was no difference in signal intensity and graft visibility between 52 and 104 weeks on MRI. At 52 and 104 weeks the graft appeared well aligned, with a hypointense signal (Fig. 2). The infusion of Gd-DTPA did not lead to a notable contrast enhancement of the graft at either time point. Histologically, the graft tissue appeared comparable with the native ACL, and immunohistochemistry showed no further changes in vascularity compared with the 24-week group.

Changes of Signal/Noise Quotient and Correlation Analysis

The signal/noise quotient of the native ACL and the graft at 52 and 104 weeks was not significantly different before and after Gd-DTPA infusion. There was a significant difference after enhancement at 6, 12, and 24 weeks ($P = 0.028$) (Fig. 6).
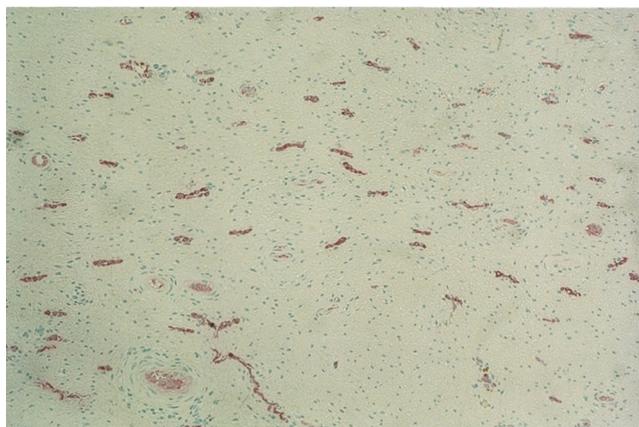
Figure 4. Vascularization of the graft tissue at 12 weeks. The graft is still hypervascular, but vessels are uniformly distributed over the entire graft cross section (transverse section, factor VIII immunostain).
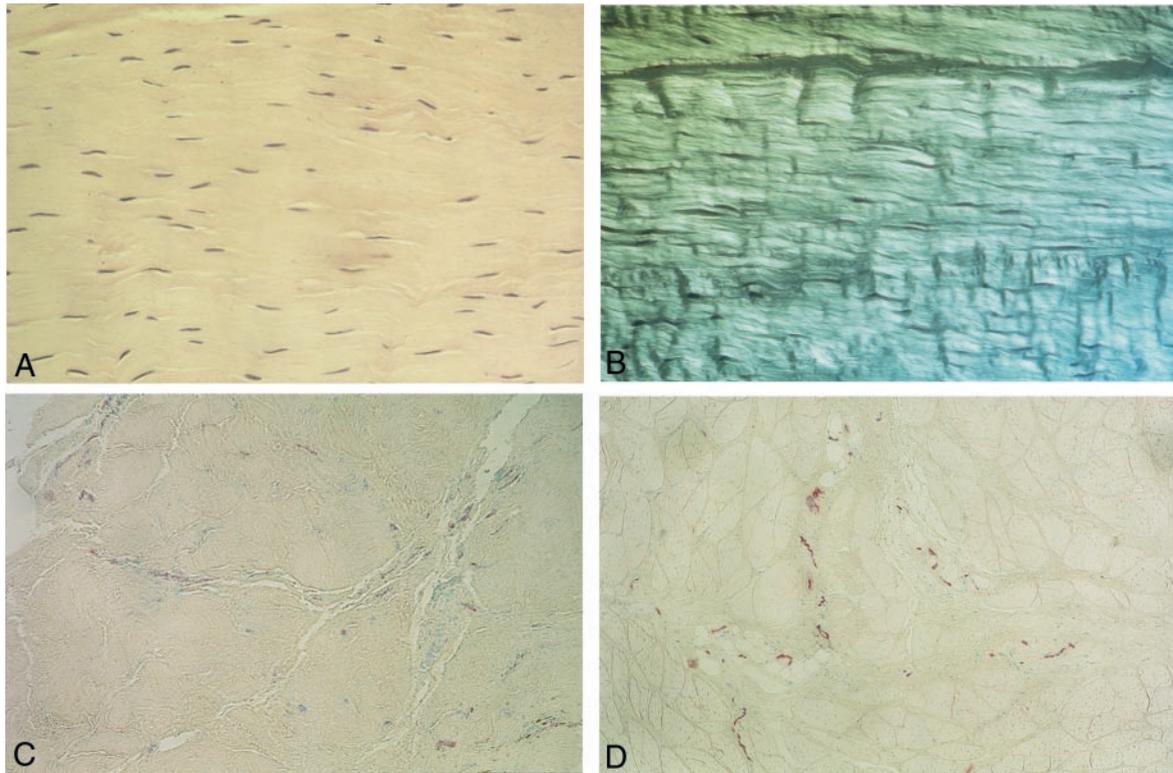
Figure 5. A, graft tissue at 24 weeks shows a normal amount of cells with fusiform fibrocysts (H&E stain, longitudinal section). B, polarized light microscopy shows a regular crimp pattern (polarized light, longitudinal section). C, factor VIII immunostain at 24 weeks shows reduced vascularity with vessels distributed between fascicles (transverse section, factor VIII immunostain). D, factor VIII immunostain of the native ACL shows a similar vascularity (transverse section, factor VIII immunostain).
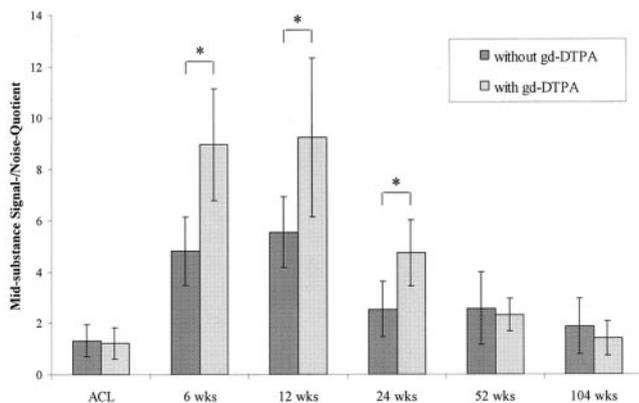
Figure 6. Changes over time in the signal/noise quotient at midsubstance with and without administration of Gd-DPTA. Data are given as means $\pm$ standard deviations. *, significant difference between pre- and postinfusion with Gd-DTPA ($P \leq$ 0.05, Wilcoxon test).

Changes in the signal/noise quotient after Gd-DTPA infusion over time showed a significantly increased signal intensity of the graft tissue at 6, 12, 24, and 52 weeks compared with the native ACL (Fig. 7A). At 104 weeks the signal/noise quotient was not significantly different from that of the native ACL. Between 6 and 12 weeks there was

no significant difference, whereas between 12 and 24 weeks the signal/noise quotient decreased significantly (Fig. 7A). The signal/noise quotient continuously decreased up to 104 weeks. Although there was no statistically significant decrease of signal/noise quotient between 24 and 52 weeks, data between 52 and 104 weeks were significantly different (Fig. 7A). Changes in the signal/noise quotient over time without Gd-DTPA enhancement showed a significantly increased signal intensity of the graft tissue only at 6 and 12 weeks compared with the native ACL (Fig. 7B). There was no significant difference between 6 and 12 weeks, whereas there was a significant decrease between 12 and 24 weeks (Fig. 7B). The decrease between 24 and 52 weeks and between 52 and 104 weeks was not statistically significant.

Correlation analyses revealed significant negative linear correlation between pre- and postinfusion signal/noise quotients and all biomechanically determined parameters (Table 2). The strongest correlations were found between tensile strength and failure load and signal/noise quotient and the weakest between stiffness and signal/noise quotient (Table 2). Without contrast enhancement, the strongest correlations were found between load to failure and tensile strength and the signal/noise quotient measured close to the tibial insertion site. With Gd-DTPA enhancement, the strongest correlations were found between tensile strength and failure load and the signal/noise quotient
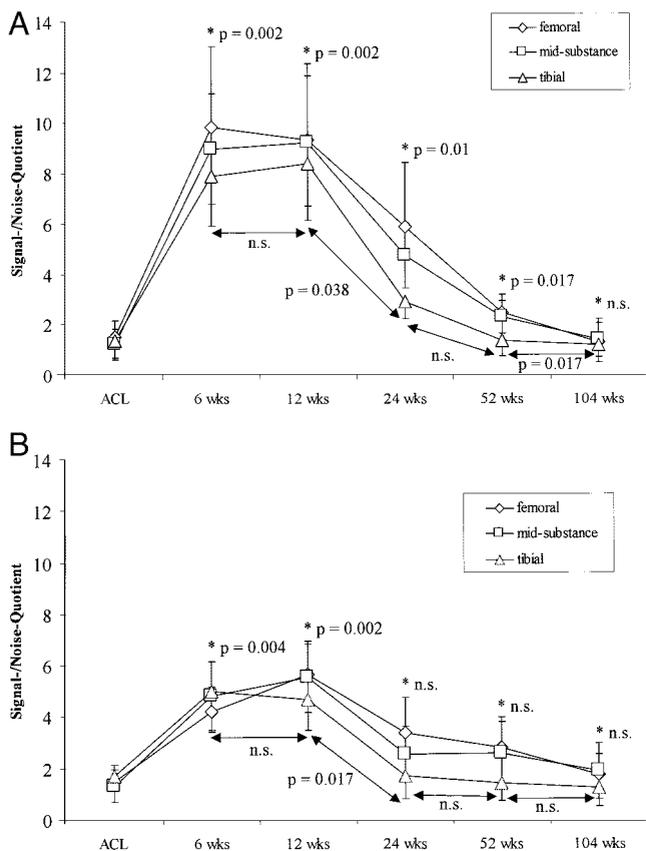
Figure 7. Changes over time in the signal/noise quotient at the three different measured locations with (A) and without (B) Gd-DTPA enhancement. Data are given as means ± standard deviations. Probability levels are given for the mid-substance location of the signal/noise quotient measurements (*, Mann-Whitney *U* Wilcoxon rank sum test between the native ACL and the corresponding study group).

TABLE 2
Results for Spearman-Rho Correlation Analysis ($\alpha = 0.05$)[a]

Variable	Load to failure	Tensile strength	Stiffness
Signal/noise quotient			
T1 Images			
Femoral	−0.606	−0.607	−0.466[b]
Midsubstance	−0.658	−0.686	−0.543[c]
Tibial	−0.733	−0.749	−0.592[d]
Gd-DTPA-enhanced Images			
Femoral	−0.736	−0.741	−0.65
Midsubstance	−0.711	−0.773	−0.642
Tibial	−0.701	−0.741	−0.617

[a] $P < 0.0001$ for all except as indicated.
[b] $P = 0.011$.
[c] $P = 0.002$.
[d] $P = 0.001$.

measured at all three measured locations (Table 2). In general, correlation coefficients between post Gd-DTPA infusion signal/noise quotient were stronger than those determined with plain imaging.

DISCUSSION

Our first research question addressed whether changes in MRI signal intensity reflect the process of graft remodeling as measured by biomechanical and histologic parameters. We found that signal intensity on preinfusion MRI scans was significantly elevated at 6 to 12 weeks. At these time periods we found the lowest tensile stress of the graft, equaling only 6.8% and 15.9%, respectively, of that of the Achilles tendon graft for time-zero tensile testing. Statistically, at 24, 52, and 104 weeks the signal/noise quotient was not significantly different from that of the native ACL. At the same times tensile stress exhibited 25.4%, 63.8%, and 58.5% of that of the Achilles tendon graft, respectively. These findings indicate that the intense signal increase in MRI reflects the severe decrease of mechanical properties during the early remodeling. On the basis of preinfusion MRI scans, it could be concluded that the return of signal intensity at 24 to 104 weeks may indicate a certain amount of structural graft restitution. In contrast to these findings, postinfusion MRI scans showed that the signal/noise quotient of the native ACL had returned only at 104 weeks. This observation may lead to the conclusion that the enhancement of Gd-DTPA refines MRI by means of more accurately detecting changes in signal intensity, thus detecting changes of structural graft properties even during the late remodeling.

The conventional histologic evaluation of the graft tissue at 6 weeks showed areas of distinctly different organization. We found areas with well-aligned hypocellular and hypovascular former graft tissue and areas with hypercellular and hypervascular reparative tissue characterized by a disorganized and loose extracellular matrix. At that time, MRI showed an inhomogeneous signal with areas of hyperintense and hypointense signal intensity. An increased signal intensity on proton-weighted MRI scans is known to represent tissue with an increased water content and a high vascularity, especially in contrast-enhanced imaging.[14,30] Thus, it may be reasonable to assume that the hypointense signal areas in MRI may represent the former nonremodeled graft tissue and that the hyperintense signal areas represent the new reparative tissue. Furthermore, changes of MRI signal intensity over time may represent the maturation process of the graft, which has been shown to be accompanied by a reduction in vascularity and water content.[23,35,41]

Our second research question addressed whether quantitative MRI parameters, such as signal intensity, predict biomechanical graft properties. We found significant negative linear correlations between all three determined biomechanical parameters and the pre- and postinfusion signal/noise quotient. In principal, this finding indicates that quantitatively determined and normalized MRI signal intensity may be useful to predict the graft's mechanical properties after ACL reconstruction and may thus be a tool to quantitatively follow the graft remodeling process in humans. However, to have a reliable tool to noninvasively study graft remodeling in humans, further variables possibly influencing MRI signal intensity have to be

identified. In the present study, the strongest correlations were found for contrast-enhanced MRI; therefore, we recommend use of a contrast medium to further study changes of signal intensity during graft remodeling over time. Although signal intensity of the graft tissue at 104 weeks had returned to normal values as compared with the native ACL, the structural properties of the graft were still inferior compared with the ACL or the graft tissue at time zero. Thus, the return to normal signal intensity may not reflect the graft tissue's absolute strength values but may indicate a certain structural restitution by means of a finished remodeling process.

To our knowledge, only a few studies have serially followed the ACL graft remodeling process by quantitatively determining MRI signal intensity.[4,48,54] Stöckle et al.[48] followed up 20 ACL reconstructions in humans over a period of 2 years. The highest signal intensity was found at 1 year, with only moderately elevated signal intensity at 3 months and poor graft visibility at up to 2 years. Thus, Stöckle et al. concluded that MRI after ACL reconstruction is a poor predictor of graft integrity after ACL reconstruction. These findings are in contrast to the data of the present experiment and a clinical study that followed ACL reconstructions with MRI.[23] However, in the study by Stöckle et al., graft impingement by the intercondylar roof was not excluded as a factor, although it has been shown to ultimately influence signal intensity of an ACL graft on MRI.[19,22] In another clinical study, conducted by Bachmann et al.,[4] 74 ACL reconstructions were followed by quantitative signal intensity measurements for up to 2 years. In this study, the highest signal intensity was found between 4 and 11 months (approximately twofold the intensity seen at 1 to 3 months). However, as in the Stöckle et al. study, graft impingement was not excluded before MRI. Wacker et al.[54] compared patellar tendon and semitendinosus tendon ACL reconstruction by MRI at 6 weeks and 6 months. They found that the signal increase in the patellar tendon group at 6 months was significantly higher compared with the hamstring tendon group, indicating that the graft choice may also influence postoperative changes in MRI signal intensity. However, the authors also found a higher rate of graft impingement in the patellar tendon group.

Our third research question addressed whether Gd-DTPA infusion improves graft visibility on MRI. We found that there were significant differences in quantitatively determined signal intensity between pre- and postinfusion MRI scans at 6 to 24 weeks. Morphologically, graft visibility was improved only at 6 and 12 weeks. At 6 weeks there was a contrast enhancement of the synovial sheet surrounding the graft, thereby increasing the contrast between the periligamentous tissue and the graft. Thus, it could be concluded that contrast-enhanced MRI is superior to plain imaging to visualize the graft after ACL reconstruction, especially in the early healing stage. From the clinical point of view, MRI offers a noninvasive tool for detecting pathologic changes in the reconstructed ACL, especially the consequence of a retrauma with respect to graft integrity. Thus, numerous clinical studies have investigated ACL graft visualization by MRI.[1,3,4,11,15,16,34,38–40,45,46,48–51,53,58]

Among these studies, however, there is still controversy about the applicability of MRI for detecting graft integrity[1,11,34,38,45,48,49,51,58] or predicting knee stability.[3,4,15,40,53]

Our fourth research question addressed whether the degree of contrast medium enhancement reflects graft vascularity on MRI. Magnetic resonance imaging combined with Gd-DTPA infusion has been shown to be comparable to histologic findings in grading vascularity in the rheumatoid knee.[30] Therefore, Gd-DTPA-enhanced imaging may also allow one to detect the vascular status of ligament tissue around the knee.[23] In fact, we found that the periligamentous contrast enhancement in MRI at 6 weeks could be explained by the increased vascularity of the synovial membrane and the subsynovial graft tissue at 6 weeks compared with the sparse intraligamentous vascularization found with immunohistochemical vessel staining. In addition, at 12 weeks there was an intense and homogeneous postinfusion contrast enhancement of the graft tissue itself, which may be due to the homogeneous vessel distribution in the center of the graft and the decrease in synovial vascularity. At 24 weeks we found no increased vascularity of the graft compared with the native ACL, although there was still a significant signal/noise quotient difference in pre- and postinfusion MRI scans. However, a limitation of the present study is that we did not determine vessel density quantitatively by means of histomorphometry. Although we found no differences between pre- and postinfusion signal/noise quotient at 52 and 104 weeks, there was still an elevated contrast enhancement at 52 weeks in the grafts compared with the native ACL. This may be attributable to the fact that minor structural changes of the graft could still be detected at that time.

Researchers using animal studies have investigated cruciate ligament autograft and allograft maturation in the past, and they reported a decrease in strength and variation in elongation of the graft over the first 9 weeks with some slight improvement in mechanical properties at 12 weeks.[2,6,8,9,13,18,26,28,35,42,59] The knowledge about the graft remodeling process resulting from these studies led to clinical recommendations with respect to the rehabilitation protocol after ACL reconstruction in humans. Besides the required protection of an ACL graft until its osseous incorporation has taken place, rehabilitation protocols mainly have focused on techniques to avoid overstraining graft tissue, thus preventing a persistent graft elongation. However, some authors have stated that the severe loss of mechanical properties after ACL replacement in laboratory animals may not be found in humans because ACL replacement in animals may not be as accurate as in humans in terms of proper orientation or tensioning. Jackson et al.[25] investigated changes of mechanical properties in an ACL in situ freezing model and found no difference in tensile strength at 6 and 26 weeks compared with the untreated control. They concluded that loss of strength may not be the natural sequela of the revascularization and healing process, and other studies have proven the detrimental effect of improper graft orientation and tensioning on the tissue's mechanical properties.[7,29,32,43]

To our knowledge, no previous studies have used an animal model to evaluate MRI signal changes during ACL graft remodeling over time; thus, no data are available comparing MRI data with histologic and, especially, biomechanical parameters. However, the data presented here may be useful in understanding the remodeling process after ACL reconstruction in humans. Radice et al. (unpublished data, 1997) compared MRI signal changes over time with histologic data from biopsy specimens taken during second arthroscopic procedures. On the basis of their histologic and MRI findings, they concluded that the graft remodeling process in humans ends at 9 months. Again, in this study, graft impingement was not excluded, and high signal intensity was found only at the midsubstance portion of the graft. On reviewing the literature, we found only one study that accurately followed the remodeling of an unimpinged ACL graft in terms of revascularization with MRI. In this study by Howell et al.[23] no difference between ACL graft and PCL signal intensity was found at any time between 1 month and 1 year. Thus, it may be reasonable to hypothesize that the extreme decrease of mechanical properties observed during the early remodeling period in previous animal studies, as well as in the present one, may not occur with the same intensity in humans, possibly because of improper graft tensioning and positioning in laboratory animals. This hypothesis could further be supported by the histologic evaluation of biopsy specimens taken during second arthroscopic procedures at different time points after hamstring tendon ACL reconstruction.[27] Johnson[27] found no gross histologic changes and concluded that the graft underwent no obvious remodeling in his patient series.

Many questions still remain concerning the influence of covariates on changes in MRI signal intensity during ACL graft remodeling and the implications such covariates may have on following the graft remodeling process in a noninvasive and accurate way. No data are available comparing MRI data with histologic and biomechanical parameters. Data on these parameters may also be useful for understanding the variables of graft remodeling after ACL reconstruction in humans. The present data may present a scientific base for comparing animal and human data with respect to possible differences in the graft remodeling process.

ACKNOWLEDGMENTS

REFERENCES

1. Allgayer B, Gradinger R, Lehner K, et al: Magnetic resonance tomography in the assessment of anterior cruciate ligament reconstruction by tendon grafts [in German]. *Rofo Fortschr Geb Röntgenstr Neuen Bildgeb Verfahr 155:* 294–298, 1991
2. Amendola A, Fowler P: Allograft anterior cruciate ligament reconstruction in a sheep model. The effect of synthetic augmentation. *Am J Sports Med 20:* 336–346, 1992
3. Autz G, Goodwin C, Singson R: Magnetic resonance evaluation of anterior cruciate ligament repair using the patellar tendon double bone block technique. *Skeletal Radiol 20:* 585–588, 1991
4. Bachmann G, Cassens J, Heinrichs C, et al: MRI of the knee in the follow-up of the plastic repair of the anterior cruciate ligament with autologous semitendinosus graft [in German]. *Rofo Fortschr Geb Röntgenstr Neuen Bildgeb Verfahr 161:* 446–452, 1994
5. Barber FA, Elrod BF, McGuire DA, et al: Preliminary results of an absorbable interference screw. *Arthroscopy 11:* 532–548, 1995
6. Bosch U, Kasperczyk WJ: Healing of the patellar tendon autograft after posterior cruciate ligament reconstruction—A process of ligamentization? An experimental study in a sheep model. *Am J Sports Med 20:* 558–566, 1992
7. Bush-Joseph CA, Cummings JF, Buseck M, et al: Effect of tibial attachment location on the healing of the anterior cruciate ligament freeze model. *J Orthop Res 14:* 534–541, 1996
8. Butler DL, Grood ES, Noyes FR, et al: Mechanical properties of primate vascularized vs. nonvascularized patellar tendon grafts: Changes over time. *J Orthop Res 7:* 68–79, 1989
9. Butler DL, Hulse D, Kay M, et al: Biomechanics of cranial cruciate ligament reconstruction in the dog. II. Mechanical properties. *Vet Surg 12:* 113–118, 1983
10. Caborn DN, Coen M, Neef R, et al: Quadrupled semitendinosus-gracilis autograft fixation in the femoral tunnel: A comparison between a metal and a bioabsorbable interference screw. *Arthroscopy 14:* 241–245, 1998
11. Cheung Y, Magee TH, Rosenberg ZS, et al: MRI of anterior cruciate ligament reconstruction. *J Comput Assisted Tomogr 16:* 134–137, 1992
12. Claes L: Empfehlung für tierexperimentelle Untersuchungen zum Bandersatz. *Hefte zu der Unfallchirurg 234:* 206–210, 1994
13. Clancy WG Jr, Narechania RG, Rosenberg TD, et al: Anterior and posterior cruciate ligament reconstruction in rhesus monkeys. *J Bone Joint Surg 63A:* 1270–1284, 1981
14. Gallimore GW Jr, Harms SE: Knee injuries: High-resolution MR imaging. *Radiology 160:* 457–461, 1986
15. Grøntvedt T, Engebretsen L, Rossvoll I, et al: Comparison between magnetic resonance imaging findings and knee stability: Measurements after anterior cruciate ligament repair with and without augmentation: A five- to seven-year followup of 52 patients. *Am J Sports Med 23:* 729–735, 1995
16. Haller W, Gradinger R, Reiser M: Results of magnetic resonance tomography (MRT) in the follow-up of transplantations of the cruciate ligament [in German]. *Unfallchirurg 89:* 375–379, 1986
17. Hamner DL, Brown CH Jr, Steiner ME, et al: Hamstring tendon grafts for reconstruction of the anterior cruciate ligament: Biomechanical evaluation of the use of multiple strands and tensioning techniques. *J Bone Joint Surg 81A:* 549–557, 1999
18. Holden JP, Grood ES, Butler DL, et al: Biomechanics of fascia lata ligament replacements: Early postoperative changes in the goat. *J Orthop Res 6:* 639–647, 1988
19. Howell SM, Berns GS, Farley TE: Unimpinged and impinged anterior cruciate ligament grafts: MR signal intensity measurements. *Radiology 179:* 639–643, 1991
20. Howell SM, Clark JA, Blasier RD: Serial magnetic resonance imaging of hamstring anterior cruciate ligament autografts during the first year of implantation. A preliminary study. *Am J Sports Med 19:* 42–47, 1991
21. Howell SM, Clark JA, Farley TE: Serial magnetic resonance study assessing the effects of impingement on the MR image of the patellar tendon graft. *Arthroscopy 8:* 350–358, 1992
22. Howell SM, Clark JA, Farley TE: A rationale for predicting anterior cruciate graft impingement by the intercondylar roof: A magnetic resonance imaging study. *Am J Sports Med 19:* 276–282, 1991
23. Howell SM, Knox KE, Farley TE, et al: Revascularization of a human anterior cruciate ligament graft during the first two years of implantation. *Am J Sports Med 23:* 42–49, 1995
24. Ihara H, Miwa M, Deya K, et al: MRI of anterior cruciate ligament healing. *J Comput Assisted Tomogr 20:* 317–321, 1996
25. Jackson DW, Grood ES, Cohn BT, et al: The effects of in situ freezing on the anterior cruciate ligament: An experimental study in goats. *J Bone Joint Surg 73A:* 201–213, 1991
26. Jackson DW, Grood ES, Goldstein JD, et al: A comparison of patellar tendon autograft and allograft used for anterior cruciate ligament reconstruction in the goat model. *Am J Sports Med 21:* 176–185, 1993
27. Johnson LL: The outcome of a free autogenous semitendinosus tendon graft in human anterior cruciate reconstructive surgery: A histological study. *Arthroscopy 9:* 131–142, 1993
28. Kasperczyk WJ, Bosch U, Oestern HJ, et al: Staging of patellar tendon autograft healing after posterior cruciate ligament reconstruction. A biomechanical and histological study in a sheep model. *Clin Orthop 286:* 271–282, 1993
29. Keira M, Yasuda K, Kaneda K, et al: Mechanical properties of the anterior cruciate ligament chronically relaxed by elevation of the tibial insertion. *J Orthop Res 14:* 157–166, 1996

30. König H, Sieper J, Wolf KJ: Rheumatoid arthritis: Evaluation of hypervascular and fibrous pannus with dynamic MR imaging enhanced with Gd-DTPA. *Radiology 176:* 473–477, 1990

31. Lee JK, Yao L, Phelps CT, et al: Anterior cruciate ligament tears: MR imaging compared with arthroscopy and clinical tests. *Radiology 166:* 861–864, 1988

32. Majima T, Yasuda K, Yamamoto N, et al: Deterioration of mechanical properties of the autograft in controlled stress-shielded augmentation procedures: An experimental study with rabbit patellar tendon. *Am J Sports Med 22:* 821–829, 1994

33. Mandelbaum BR, Finerman GAM, Reicher MA, et al: Magnetic resonance imaging as a tool for evaluation of traumatic knee injuries: Anatomical and pathoanatomical correlations. *Am J Sports Med 14:* 361–370, 1986

34. Maywood RM, Murphy BJ, Uribe JW, et al: Evaluation of arthroscopic anterior cruciate ligament reconstruction using magnetic resonance imaging. *Am J Sports Med 21:* 523–527, 1993

35. McFarland EG, Morrey BF, An KN, et al: The relationship of vascularity and water content to tensile strength in a patellar tendon replacement of the anterior cruciate in dogs. *Am J Sports Med 14:* 436–448, 1986

36. McGuire DA, Barber FA, Elrod BF, et al: Bioabsobable interference screws for graft fixation in anterior cruciate ligament reconstruction. *Arthroscopy 15:* 463–473, 1999

37. Mink JH, Levy T, Crues JV III: Tears of the anterior cruciate ligament and menisci of the knee: MR imaging evaluation. *Radiology 167:* 769–774, 1988

38. Moeser P, Bechtold RE, Clark T, et al: MR imaging of anterior cruciate ligament repair. *J Comput Assisted Tomogr 13:* 105–109, 1989

39. Munk PL, Vellet AD, Fowler PJ, et al: Magnetic resonance imaging of reconstructed knee ligaments. *Can Assoc Radiol J 43:* 411–419, 1992

40. Murakami Y, Sumen Y, Ochi M, et al: MR evaluation of human anterior cruciate ligament autograft on oblique axial imaging. *J Comput Assisted Tomogr 22:* 270–275, 1998

41. Ng GY, Oakes BW, Deacon OW, et al: Long-term study of the biochemistry and biomechanics of anterior cruciate ligament-patellar tendon autografts in goats. *J Orthop Res 14:* 851–856, 1996

42. Ng GY, Oakes BW, Deacon OW, et al: Biomechanics of patellar tendon autograft for reconstruction of the anterior cruciate ligament in the goat: Three-year study. *J Orthop Res 13:* 602–608, 1995

43. Ohno K, Yasuda K, Yamamoto N, et al: Effects of complete stress-shielding on the mechanical properties and histology of in situ frozen patellar tendon. *J Orthop Res 11:* 592–602, 1993

44. Polly DW Jr, Callaghan JJ, Sikes RA, et al: The accuracy of selective magnetic resonance imaging compared with the findings of arthroscopy of the knee. *J Bone Joint Surg 70A:* 192–198, 1988

45. Rak KM, Gillogly SD, Schaefer RA, et al: Anterior cruciate ligament reconstruction: Evaluation with MR imaging. *Radiology 178:* 553–556, 1991

46. Rose NE, Gold SM: A comparison of accuracy between clinical examination and magnetic resonance imaging in the diagnosis of meniscal and anterior cruciate ligament tears. *Arthroscopy 12:* 398–405, 1996

47. Shellock FG, Mink JH, Curtin S, et al: MR imaging and metallic implants for anterior cruciate ligament reconstruction: Assessment of ferromagnetism and artifact. *J Magn Reson Imaging 2:* 225–228, 1992

48. Stöckle U, Hoffmann R, Schwedtke J, et al: Value of MRI in assessment of cruciate ligament replacement [in German]. *Unfallchirurg 100:* 212–218, 1997

49. Tosch U, Hertel P, Bernard M, et al: Gadolinium-DTPA gestützte MRT zur Beurteilung des Einheilens von autologen Ligamentum-patellae-Transplantaten als vorderer Kreuzbandersatzplastik. *Radiologe 33:* 40–45, 1993

50. Tosch U, Sander B, Schubeus P, et al: An NMR tomographic follow-up assessment of the replacement plastic repair of the anterior cruciate with autologous ligamentum patellae transplant [in German]. *Rofo Fortschr Geb Röntgenstr Neuen Bildgeb Verfahr 153:* 716–720, 1990

51. Trieshmann HW Jr, Mosure JC: The impact of magnetic resonance imaging of the knee on surgical decision making. *Arthroscopy 12:* 550–555, 1996

52. Turner DA, Prodromos CC, Petasnik JP, et al: Acute injury of the ligaments of the knee: Magnetic resonance evaluation. *Radiology 154:* 717–722, 1985

53. Uhl M, Schmidt C, Riedl S, et al: Postoperative MRI morphology of the anterior cruciate ligament after primary ligament suture or ligament plasty: A prospective study of 50 patients [in German]. *Aktuelle Radiol 6:* 13–18, 1996

54. Wacker F, Schilling A, Dihlmann SW, et al: MR tomography in autologous plastic repair of the anterior cruciate ligament: A comparison of 2 surgical methods [in German]. *Rofo Fortschr Geb Röntgenstr Neuen Bildgeb Verfahr 162:* 51–57, 1995

55. Weiler A, Hoffmann RF, Stähelin AC, et al: Hamstring tendon fixation using interference screws: A biomechanical study in calf tibial bone. *Arthroscopy 14:* 29–37, 1998

56. Weiler A, Peine R, Pashminek-Azar A, et al: Tendon healing in a bone tunnel. Part I. Biomechanical results after biodegradable interference fit fixation in a model of ACL reconstruction in sheep. *Arthroscopy, in press,* 2001

57. Weiler A, Windhagen HJ, Raschke MJ, et al: Biodegradable interference screw fixation exhibits pull-out force and stiffness similar to titanium screws. *Am J Sports Med 26:* 119–128, 1998

58. Yamato M, Yamagishi T: MRI of patellar tendon anterior cruciate ligament autografts. *J Comput Assist Tomogr 16:* 604–607, 1992

59. Zimmermann MC, Contiliano JH, Parsons JR, et al: The biomechanics and histopathology of chemically processed patellar tendon allografts for anterior cruciate ligament replacement. *Am J Sports Med 22:* 378–386, 1994